Robotica (2000) volume 18, pp. 153–161. Printed in the United Kingdom © 2000 Cambridge University Press

Localization using infrared beacons

Eric Brassart, Claude Pegard, Mustapha Mouaddib

GRACSY. Groupe de Recherche sur l'Analyse et la Commande des SYstèmes, Université de Picardie Jules Verne, Amiens, France; IUT, Département Informatique, Avenue des facultés 80000 Amiens (France). E-mail: Eric.Brassart@.u-picardie.fr

(Received in Final Form: June 25, 1999)

SUMMARY

In this paper, we deal with a localization system allowing one to determine the position and orientation of a mobile robot. This system uses active beacons distributed at the ceiling of the navigation area. These beacons can transmit a coded infrared signal which allows the robots to identify the sender. A CCD camera associated to an infrared receiver allows one to compute the position with a triangulation method which needs reduced processing time. Calibration and correcting distortion stages are performed to improve accuracy in the determination of the position. Dynamic localisation is established for most actual mobile robots used in indoor areas.

KEYWORDS: Infrared beacons; Localization system; Triangulation method

1. INTRODUCTION

Localisation is one of the main functions which allows mobile robots to navigate while respecting elementary safety rules and improving autonomy. It must be particularly precise for path generation or accosting tasks in an industrial environment. Hence, the position determination of mobile robots remains a topic for which much research is carried out to find new methods and new sensors.[1–3]

Relative localization sensors are widely used in mobile robotics. The main advantages of these sensors (coding wheels, tachymeters, odometers) are easy setting in vehicles, fast determination of robot parameters with only a non-sophisticated computer, low cost, and to finish with, no equipment in the navigation area is required. They can give good results on short routes with a precision of a few percents. In long routes (>10 meters) the accumulation of drifts can lead to errors of over 10% in relative localization. Hence, a robot cannot use only relative localization to perform complex tasks.

Absolute localisation systems permit one to make periodical checkings[4] in order to correct these cumulative errors.

In fact, both systems are used on most current robots.[5] Ultrasonic sensors,[6] stereovision, dynamic vision[4] and lasers are currently used, especially for the localization stage.

In our study, we propose a 2D absolute localization system, based on a beacon-structured environment for indoors use. Infrared coded beacons are placed at the ceiling and a database giving the location of each beacon with its respective infrared code is supplied to the robots.

2. INFRARED CODED BEACON CONCEPTS

The localization system is made of two parts. The first is distributed in the navigation area. It can be used by our robot[7] in the navigation stage; the second part is placed on-board the robot in order to give it the information of localization.

2a. The marked out area

A network made of infrared beacons is placed on the ceiling of the indoor area. The three-dimensional coordinates of each beacon are incorporated into the robots.

A beacon is composed of three infrared LEDs showing an orthogonal reference (Figure 1).

We have chosen this configuration, with three LEDs making an orthogonal co-ordinate system, to spare the robot any ambiguity in position determination. Therefore, this configuration permits us to simplify image processing. Hence, when we have localized the first LED, we search for

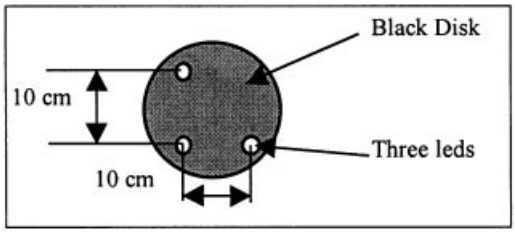

Fig. 1. An infrared beacon

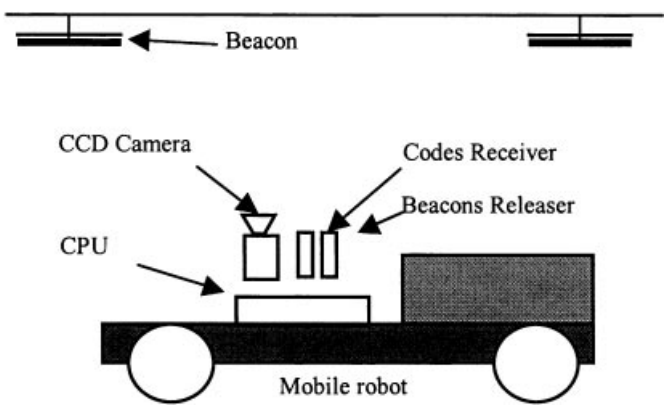

Fig. 2. Experimental platform

https://doi.org/10.1017/S0263574799001927 Published online by Cambridge University Press

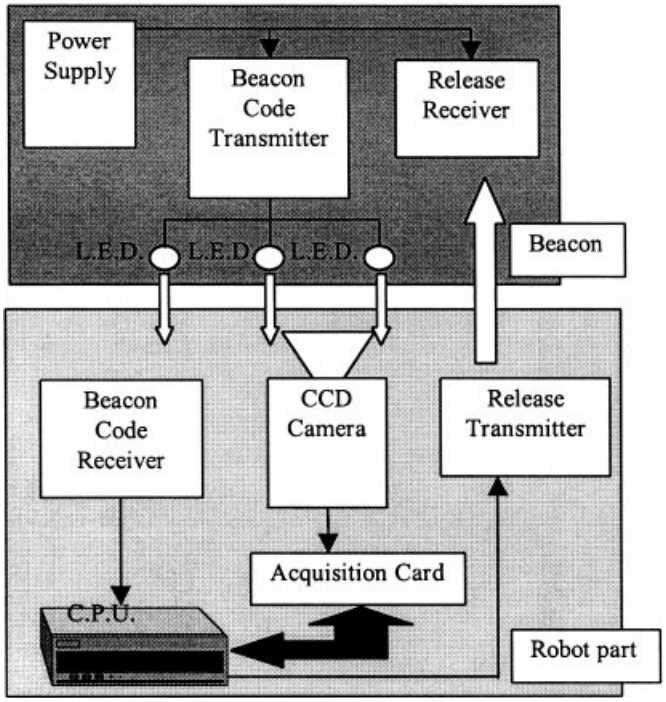

Fig. 3. Working principle

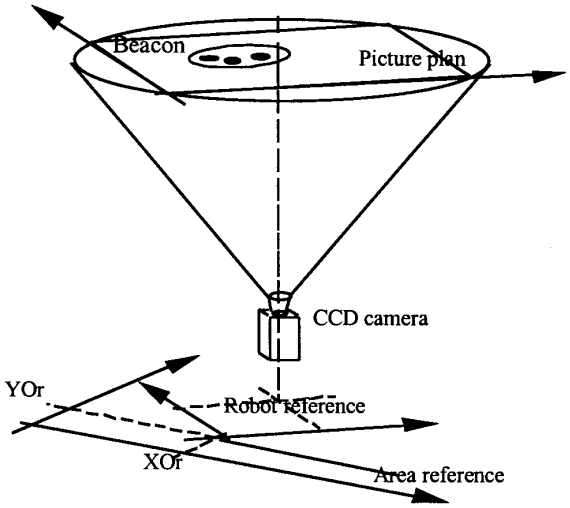

Fig. 4. Main references

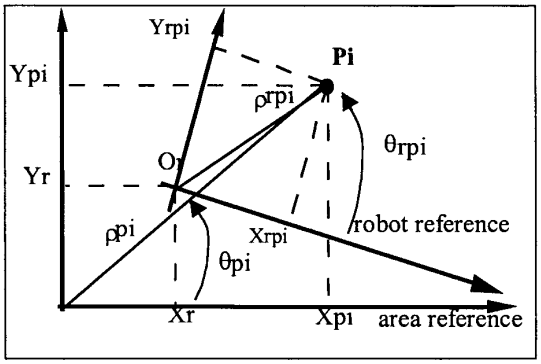

Fig. 5. Writing convention

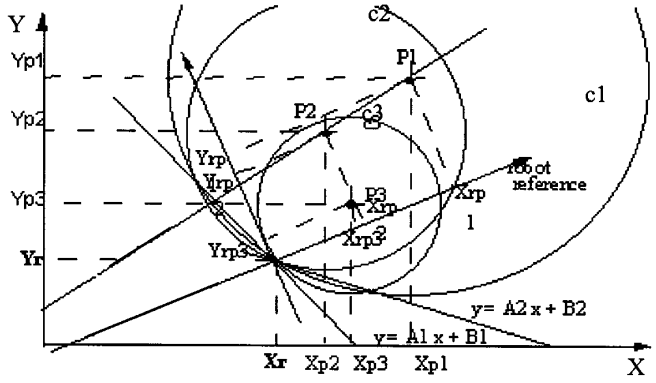

Fig. 6. Localization with 3 points

the other ones in particular narrow areas of the view; it makes the identification of the reference given by the three LEDs easy.

The gap of 10 cms between two LEDs has been chosen taking into account the physical characteristics of the camera and the mean distance between the beacons and the camera. We must obtain three distinct image points in each view.

A beacon can be released by a robot. A released beacon transmits a specific infrared code allowing the robot to know its identifier. The beacon number associated with the camera picture gives an absolute localization. Only one beacon must be seen in a picture. Good visibility and a sufficient density are required for real-time localization.

2b. Robot equipment

An infrared transmitter controls the release of the beacons. A vertically oriented CCD camera allows one to see one beacon at the most. An infrared receiver is used to determine the beacon identifier (Figures 2 and 21) These three parts are controlled by an Intel CPU.

2c. Working principle

It is based on the conjointed use of two sensors: a CCD camera and an infrared receiver (Figure 3).

A beacon releaser is able to transmit an infrared signal which can be received by the nearest beacon. This beacon is activated for 0.2 sec. As soon as a release signal has been transmitted, a picture is captured by the CCD camera and a beacon identification code is received. Frequency shift keying modulation (FSK) is used for faultness identification code transmission. This modulation, uses three frequencies: 1200 Hertz and 1600 Hertz for the logical level (0 and 1), which identify the beacon code, and a carrier frequency of 40 000 Hertz, which has no effect on the CCD camera working with a low frequency (35 Hertz). As soon as the code of the beacon has been identified and the receiver has detected the first code, an image is taken and image processing begins.

This localization system can be used simultaneously by several robots. The number of beacons distributed in the navigation area depends on the size of the coded binary word. In our case, generated codes for identification are made with 8 bits.

https://doi.org/10.1017/S0263574799001927 Published online by Cambridge University Press

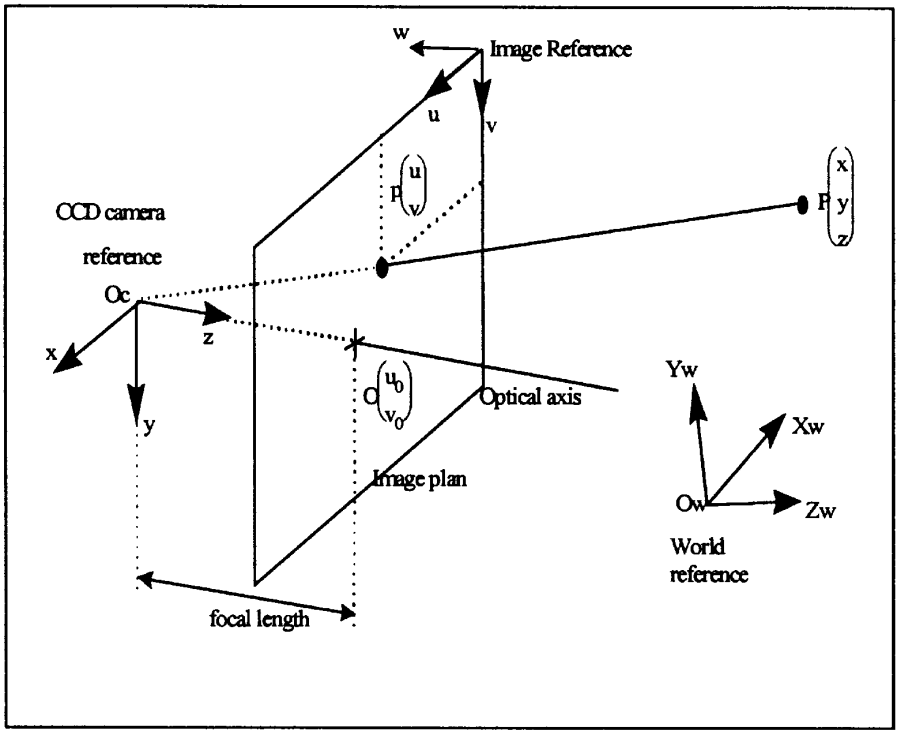

Fig. 7. Camera model

2d. Coordinates determination

The CCD camera is supposed to be vertically oriented. Only one beacon is seen in the camera field. The captured picture associated with the beacon code and geometric computation allow one to know the absolute co-ordinates and orientation (Figure 4).

Two references are available: a stationary area reference and a mobile robot reference. A p_i point has Xp_i, Yp_i coordinates in the area reference, and, Xrp_i, Yrp_i coordinates in the robot reference (Figure 5).

We have to determine the position and orientation of the robot reference origin in navigation area. A beacon is composed of three infrared LEDs which constitute three observed points.

For each point, a modulus and an argument can be computed in the two references. These six basic data allow us to know the precise position of the robot in the area. The method consists of searching the intersection of three circle of p_i center and $\rho r p_i$ observed radius with i-1,2,3 [Figure 6].

Equations of the circles are:

$$(x - Xp_i)^2 + (y - Yp_i)^2 - rrp_i^2 = 0 \text{ for } c_i$$

with $i = 1,2,3$

The equation of the line going through the intersections of c_a and c_b is:

$$A_n x + B_n Y = C_n \quad (1)$$

with $A_n = 2*(Xp_b - Xp_a)$; $B_n = 2*(Yp_b - Yp_a)$

$$C_n = -Xp_a^2 + Xp_b^2 - Yp_a^2 + Yp_b^2 + Xrp_a^2 - Xrp_b^2 + Yrp_a^2 - Yrp_b^2$$

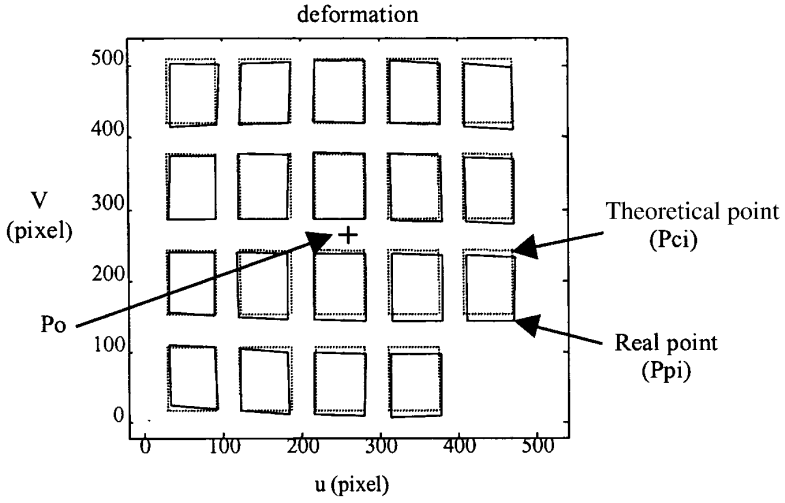

Fig. 8. Points of the theoretical squares and the calculated squares

https://doi.org/10.1017/S0263574799001927 Published online by Cambridge University Press

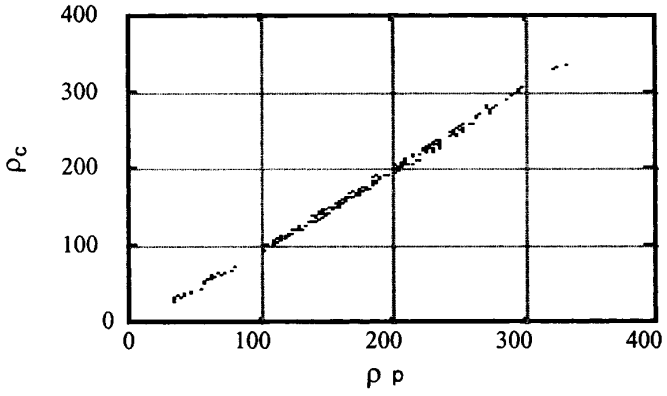

Fig. 9. Curve $\rho c = f\,\rho p$)

where a = 1, 1, 2; b = 2, 3, 3; n = 1, 2, 3

These three lines (1) are concurrent at the robot refrence origin, hence the robot coordinates are:

$$\mathrm{yr_j} = \frac{\mathrm{C_b} - \mathrm{A_b}\beta_a}{\mathrm{A_b}\ \alpha_a + \mathrm{B_b}}$$

$$\mathrm{xr_j} = \alpha_a \frac{\mathrm{C_b} - \mathrm{A_b}\beta_a}{\mathrm{A_b}\ \alpha_a + \mathrm{B_b}} + \beta_a$$

with

$$\alpha_a = -\frac{B_a}{A_a} \text{ and } \beta_a = \frac{C_a}{A_a}$$

and respectively when j = 1, 2, 3 a = 1, 1, 2; b = 2, 3, 3

Thus, we obtain three results for the localization, generally nearest, and the final result is calculated by taking the mean of the robot reference origin:

$$\mathrm{xr} = \overline{\mathrm{xr}_i}$$
$$\mathrm{yr} = \overline{yr_i}$$

Angle determination: The orientation angle is computed by determining the angular gap between two lines, tied to each reference, going through the same couple of points.

$$\theta \mathrm{r_j} = \mathrm{atan}\,\frac{\mathrm{Yrp_b} - \mathrm{Yrp_a}}{\mathrm{Xrp_b} - \mathrm{Xrp_a}}$$

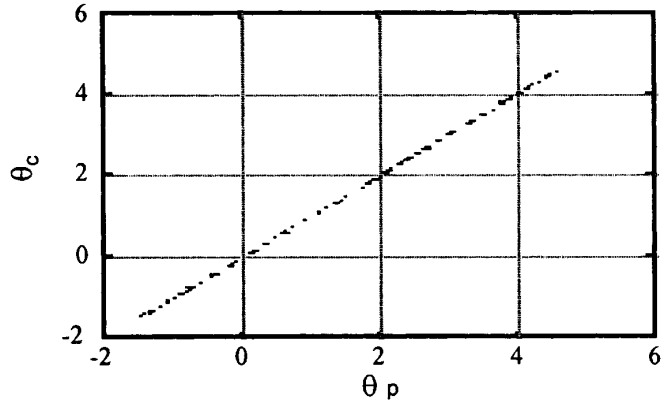

Fig. 10. Curve $\theta c = g(\theta p)$

$$\theta_j = \mathrm{atan}\,\frac{\mathrm{Yp_b} - \mathrm{Yp_a}}{\mathrm{Xp_b} - \mathrm{Xp_a}}$$

$$\text{Orientation} = \theta_j - \theta \mathrm{r_j} = \mathrm{atan}\,\frac{\mathrm{Yp_b} - \mathrm{Yp_a}}{\mathrm{Xp_b} - \mathrm{Xp_a}} - \mathrm{atan}\,\frac{\mathrm{Yrp_b} - \mathrm{Yrp_a}}{\mathrm{Xrp_b} - \mathrm{Xrp_a}}$$

Calibration stage. We have chosen to divide the calibration into two stages. At first, we have to find the perspective transformation matrix without distortion, and, next, to compute the parameters to correct radial distortion.

In order to compute an accurate position of the robot, we need to determine the precise parameters of the camera used in our application. Thus we have to determine the intrinsic and extrinsic parameters.

Intrinsic parameters define features of the sensor; extrinsic parameters correspond to rigid body transformation.[8]

Building of the camera model The CCD camera used for this application is a pinhole one. The points of the CCD matrix are obtained according to a perspective projection. Thus, from the model of the camera and from points obtained in the reference we can find an estimation of image points in the CCD reference; this stage is called calibration.

The relations linking the 3D points (xwi, ywi, zwi) and the projected points in the image reference (ui,vi) are given by a 3*4 matrix in homogeneous co-ordinates as :

$$\begin{pmatrix} Su \\ Sv \\ S \end{pmatrix} = M \begin{pmatrix} X_w \\ Y_w \\ Z_w \\ 1 \end{pmatrix} \qquad 1.1$$

where M represents intrinsic and extrinsic parameters. Hence:

$$\begin{pmatrix} Su \\ Sv \\ S \end{pmatrix} = M_{\mathrm{int}}\, M_{ext} \begin{pmatrix} X_w \\ Y_w \\ Z_w \\ 1 \end{pmatrix} = \begin{pmatrix} \alpha_u & 0 & u_0 & 0 \\ 0 & \alpha_v & v_0 & 0 \\ 0 & 0 & 0 & 0 \end{pmatrix} \begin{pmatrix} r_1 & t_x \\ r_2 & t_y \\ r_3 & t_z \\ 0 & 1 \end{pmatrix} \begin{pmatrix} X_w \\ Y_w \\ Z_w \\ 1 \end{pmatrix}$$

$$= \begin{pmatrix} m_{11} & m_{12} & m_{13} & m_{14} \\ m_{21} & m_{22} & m_{23} & m_{24} \\ m_{31} & m_{32} & m_{33} & m_{34} \end{pmatrix} \begin{pmatrix} X_w \\ Y_w \\ Z_w \\ 1 \end{pmatrix} \qquad 1.2$$

with $\alpha_u = \mathrm{k_u}\ \mathrm{f}$ and $\alpha_v = \mathrm{k_v}\ \mathrm{f}$.

There are four intrinsic parameters: u_0, v_0 which represent the projection of the optical axis on the pixel matrix,

$\frac{1}{k_u}$ and $\frac{1}{k_v}$ which correspond, respectively, to the

horizontal and vertical sizes (in m) of a CCD cell and six extrinsic parameters which characterize the rigid motion allowing to pass from the camera reference to the world reference (see 1.3 and Figure 7))

t_x, t_y, t_z for the translations

r_x, r_y, r_z for the rotations

https://doi.org/10.1017/S0263574799001927 Published online by Cambridge University Press

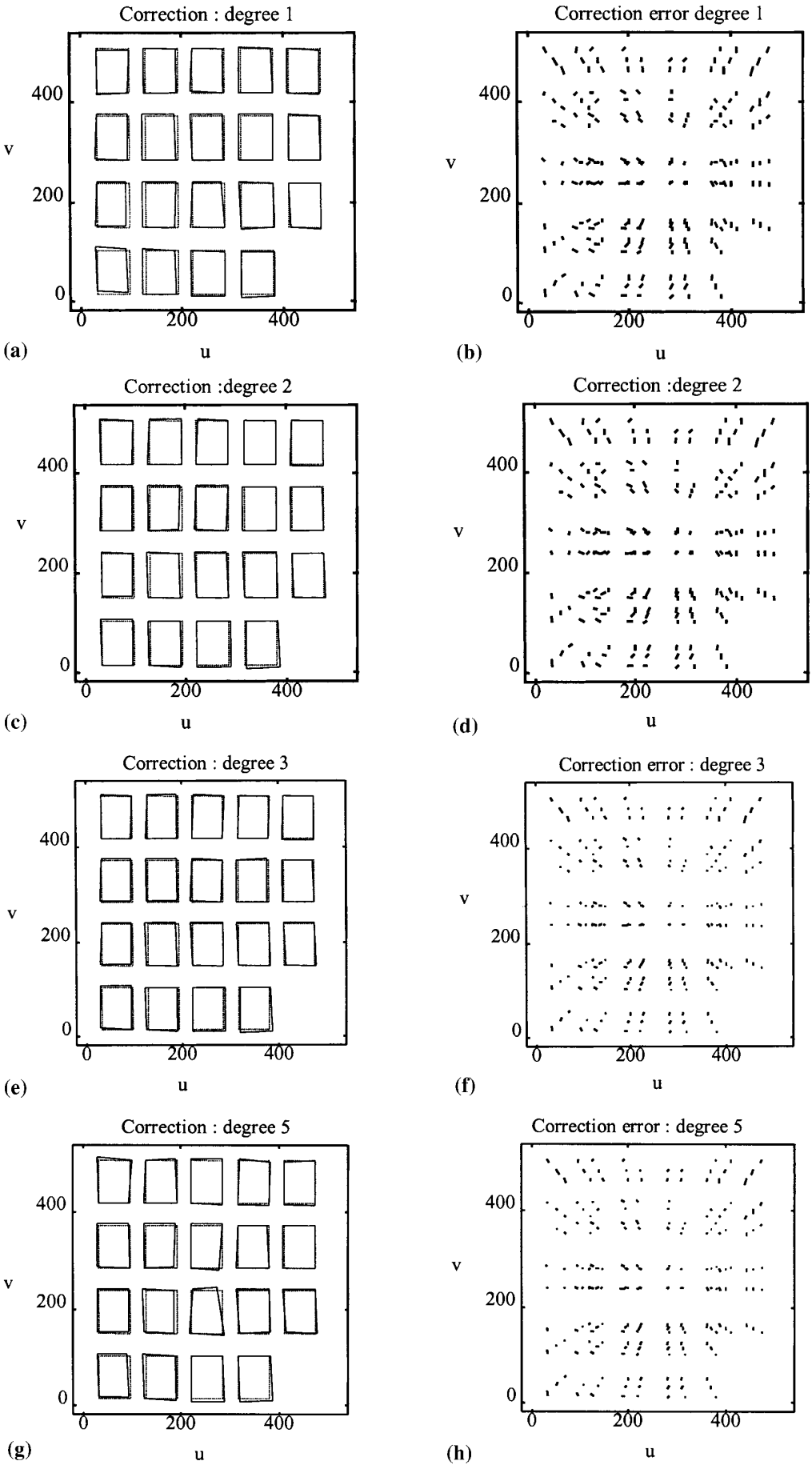

Fig. 11 (a)-(h). Results obtained with different degrees of polynomial

https://doi.org/10.1017/S0263574799001927 Published online by Cambridge University Press

$$\begin{pmatrix} x \\ y \\ z \end{pmatrix} = R \begin{pmatrix} X_w \\ Y_w \\ Z_w \end{pmatrix} + t = \begin{pmatrix} r_{11} & r_{12} & r_{13} & t_x \\ r_{21} & r_{22} & r_{23} & t_y \\ r_{31} & r_{32} & r_{33} & t_z \\ 0 & 0 & 0 & 1 \end{pmatrix} \begin{pmatrix} X_w \\ Y_w \\ Z_w \\ 1 \end{pmatrix} \quad (1.3)$$

Determination of the perspective transformation matrix. In order to compute the camera model and the parameters of distortion, we have used a micro displacement table to move our camera and to catch images of a test card made of twenty black squares on a white background. The test card is set perpendicularly to the focal axis.

Several views are taken in several planes to compute the M matrix according to the 3D points and their associated projected points with a linear solving method proposed by Faugeras and Toscani.[9,10] Thus we can give a first estimate of u_0, v_0, α_u, α_v, t_x, t_y, t_z, r_1, r_2, r_3.

In a second stage, we compute from these parameters and

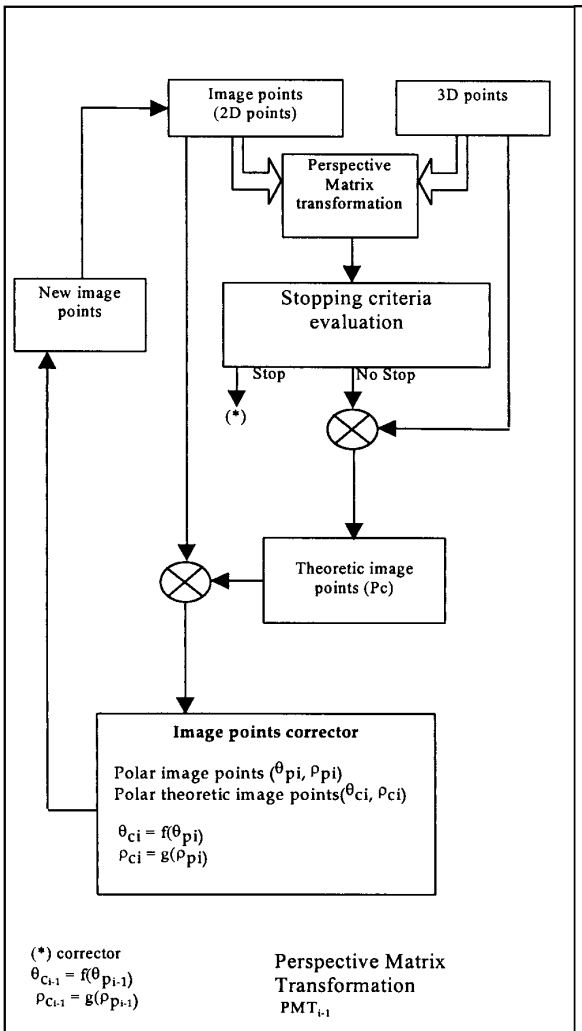

Fig. 12. Pseudo-algorithm

1 Compute the perspective matrix transform (PMT) from a set of 3D points and their corresponding projected points in the image plan (P_2D).

2 Compute the theoretical 2D points corresponding to the 3D points considering a perfect camera model using intrinsic and extrinsic parameters extracted from of the PMT.

3 Calculate from the real and the theoretical image points, ρ and θ polynomial functions and compute the new image points.

4 Determine, from the new 2D image points and their corresponding 3D points, the new perspective matrix transform, and repeat the 2, 3, 4 steps up to satisfy a stopping criteria.

Fig. 13. Algorithm

Table I. Numerical results of the intrinsic parameters

	1st iteration 1	2nd iteration 2	3rd iteration	4th iteration	5th iteration
u_0	256.09	259.24	259.43	259.45	259.46
v_0	267.38	274.60	275.26	275.33	275.34
α_u	409.06	395.48	395.39	395.36	395.34
α_v	579.14	561.67	561.65	561.62	561.61

https://doi.org/10.1017/S0263574799001927 Published online by Cambridge University Press

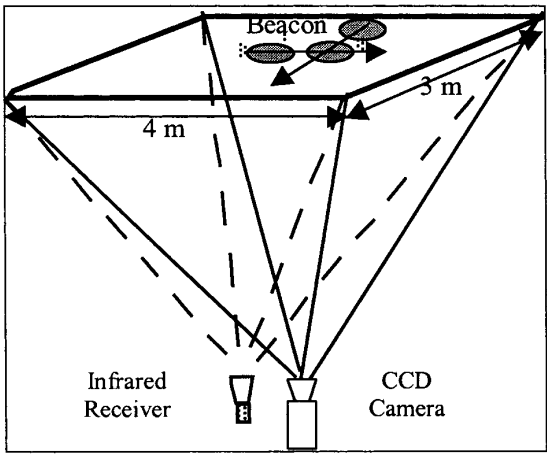

Fig. 14. Technical constraints

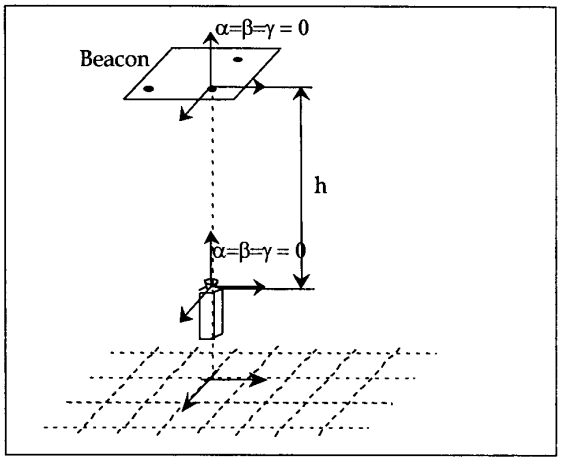

Fig. 15. Geometrical constraints

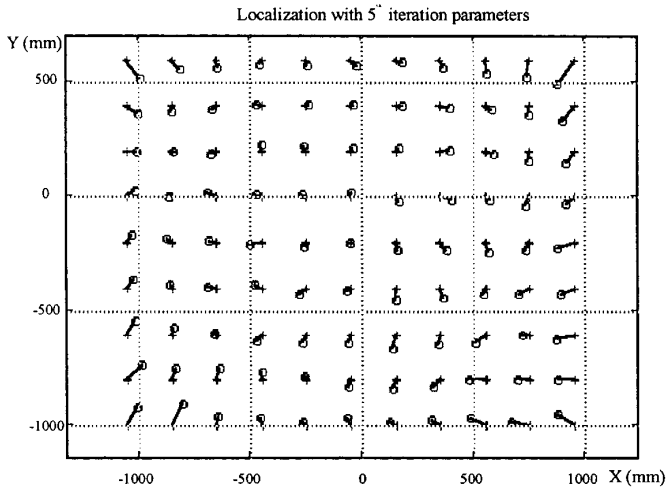

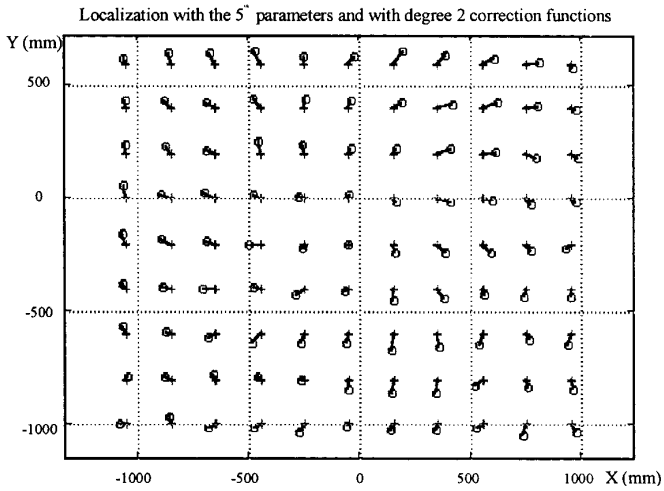

Circles represent real localization points and crosses the corrected localization points

Fig. 16. Results of localization

Fig. 17. Results of localization

Table II. Numerical results of the error localisation

Parameters	Initial PMT_1	5th Iteration (PMT_{i-1})			
Correction $\rho c = f(\rho p)$ $\theta c = g(\theta p)$	Without	Without	1st degree	2nd degree	3rd degree
Mean error X (mm)	116.51	33.55	23.60	22.57	22.45
Mean error Y (mm)	59.43	34.67	26.33	23.65	23.90

https://doi.org/10.1017/S0263574799001927 Published online by Cambridge University Press

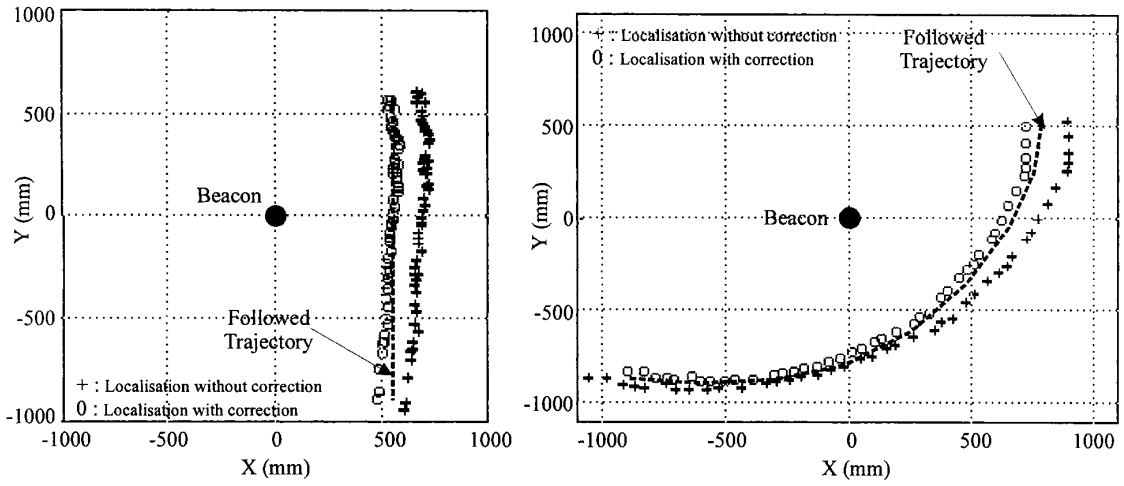

Fig. 18. Real trajectories with absolute localization

from the 3D points of the scene the u_c v_c coordinates which we call computed points. Thus we can compare two sets of points:

- the real projected points P_p (u_p, v_p)
- the computed points P_c (u_c, v_c)

From these two sets of points, we can compute the distortion model.

In order to increase the accuracy of the matrix parameters, we have used an iterative process allowing one to compute P_c.

Hence we define (Figure 8):
$P_0 = (u_0, v_0)^t$ the position of the optical centre in the image,
$Pp_i = (up_i, vp_i)^t$ the real projection in the image of a corner got in a square,
$Pc_i = (uc_i, vc_i)^t$ the theoretic projection in the image of square corners with a perfect camera model.

We define distances and angular measures :

$$\rho c_i = \sqrt{(u_0 - uc_i)^2 + (v_0 - vc_i)^2} \qquad \Theta c_i = \widehat{P_0 P c_i} \qquad 1.4$$

$$\rho p_i = \sqrt{(u_0 - up_i)^2 + (v_0 - vp_i)^2} \qquad \Theta p_i = \widehat{P_0 P p_i} \qquad 1.5$$

and we interpolate the points of figures 9 and 10 by polynomial functions:

$$\rho c = f(\rho p) \qquad 1.6$$

$$\theta c = g(\theta p) \qquad 1.7$$

Hence we can write 1.6 and 1.7 in matrix form:

$$[\rho c] = \rho_p^n \quad \rho_p^{n-1} \ldots \rho_p^0] \begin{pmatrix} a_n \\ a_{n-1} \\ \ldots \\ a_0 \end{pmatrix} \qquad 1.8$$

$$[\theta c] = \theta_p^n \quad \theta_p^{n-1} \ldots \theta_p^0] \begin{pmatrix} b_n \\ b_{n-1} \\ \ldots \\ b_0 \end{pmatrix} \qquad 1.9$$

With graphics obtained in Figures 9 and 10 we can use polynomial approximate to a weak degree to reach the points. Experience shows that the best results are obtained with a polynomial function with degrees 3 or 4. Beyond these degrees, the corrected images degrade quickly. Some results are shown in Figure 11(a)-(g). The left column (a), (c), (e), (g) gives the mark-up reconstruction from 3D points. Red squares represent the theoretical perfect mark-up, while the yellow squares represent the calculated mark-up from 1.8 and 1.9. The right column in (b), (d), (f), (h) represent error vectors between similar vertices.

Improvement of the calibration process. The accuracy can be improved by an iterative computation of the calibration process which allows one to make the results converge to a stop criterion representating a minimal variation between the i and i+1 iterations. We can find the pseudo-algorithm shown in Figures 12 and 13 describing the method used to determine the perspective transformation matrix.

The stopping criteria can be expressed in the following form:

$$(|uo_{i-1} - uo_i| < \varepsilon u_0) \text{ AND } (|vo_{i-1} - vo_i| < \varepsilon v_0) \text{ AND}$$
$$(|\alpha u_{i-1} - \alpha u_i| < \varepsilon \alpha_u) \text{ AND } (|\alpha v_{i-1} - \alpha v_i| < \varepsilon \alpha_V) \qquad 1.10$$

With:

$$\varepsilon u_0 = 0{\cdot}1 \quad \varepsilon v_0 = 0{\cdot}1 \quad \varepsilon \alpha_u = 0{\cdot}25 \quad \varepsilon \alpha_v = 0{\cdot}25 \qquad (1)$$

The obtained results are given in Table I. This array shows that only a few interations are necessary to stop the process. Only results of the intrinsic parameters obtained in the 5th iteration will be used in the next section to localise the mobile robot with our system. The residual error will be approximated by a polynomial function.

3. EXPERIMENTAL RESULTS

The first tests have been achieved with 660 nm infrared LEDs and a CCD camera of a spectral domain extending from 440 nm to 1100 nm without a filter. For our experimentation, beacons have been implanted in the same plane. The main difficulty is to make the reception field of the infrared receiver to be in the camera field (Figure 14), so

https://doi.org/10.1017/S0263574799001927 Published online by Cambridge University Press

a specially shaped by collector is used on the infrared receivers.

Beacons are separated from the robots by a distance of three meters. A 6 mm lens allows one to cover a surface of about 12 m^2.

For the experimentation, we have chosen measurement points with a precision which permit us to test our method with our developed algorithms (see Figure 15). The goal is to check how useful each camera parameter is as regards the localization of the robot, and, how the polynomial correction functions we used can improve results.

In the test area we have established which initial intrinsic parameters of the camera have to be used. The mean error localisation represents on average 6 percent in X and 4 percent in Y. If we had used parameters camera obtained for the 5^{th} iteration (Table I) of our process, with the same data, the mean error would have represented 1.6% in X and 2.3% in Y. These results can be improved using polynomials functions $\pi\tau$ and we obtain localisation errors of 1% in X $\rho\theta$ and 1.5% in Y (Figs. 16 and 17). The best results use polynomial functions with a 2^{nd} degree (table II).

Results are summarised in Table II. They show that using polynomials function 1.8 and 1.9 of a second degree, combined with the interative process described in Figure 12, we obtain the best results. Similar results are given in Figures 14 and 15 for different configurations.

We have dynamically tested our method on trajectories shown in Figure 18. Dashed points represent the real trajectory, crosses show the localization with the rough calibration method, and circles the localization with our polynomial and iterative methods.

4. CONCLUSION

Some localization techniques, currently used, are based on passive beacons, like common object shapes[11] or bar codes[12] (Caterpillar process).

We have chosen an infrared transmission associated with monocular vision to obtain good reliability in industrial plants. The process has a low sensitivity to external disturbances and gives accurate results. This system could be particularly interesting, in store-rooms or industrial plants, when light is too weak to use passive visual perception. Its use is without human risks contrary to the use of high power lasers.

The same network of infrared beacons can be easily used by several mobile robots without modification. The main disadvantage of the system is that one must hang the beacons on the ceiling. A beacon is activated for a short period of about 200 ms. Vigil periods need only a low power, so photovoltaic cells could be used to refill cadmium-nickel accumulators.

The dynamical behaviour of vehicles affects measurements; this has not been studied in this paper.

References

1. Shu-Yuan Chen and Wen-Hsiang Tsai, "Determination of robot locations by common object shapes" *IEEE Transactions on Robotics and Automation*, **7**, No. 1, 149–156 (Feb., 1991).
2. O. Faugeras, *"Three Dimensional Computer Vision: a Geometric Viewpoint"*, (MIT press, Cambridge, Mass, 1993).
3. P. Bonnifait, "Localisation précise en position et attitude des robots mobiles d'extérieurs à évolutions lentes". *PhD thesis* (Ecole Centrale de Nantes, November 1997).
4. M. Mouaddib, "Programmation, génération de trajectoires et recalages pour le R.M.A. SARAH" (in French), *Ph.D. Thesis* (University of Picardie, France, March 1991.0
5. A. Preciado Ruiz, D. Meizel, A. Segovia and M. Rombaut, "Fusion of multi-Sensor Data: a geometric approach", *Proc. IEEE Int. Conf. Robotics and Automation* (1991 pp. 2806–2811.
6. M. Drumheller, "Mobile robot localization using sonar", *A. I. Memo 826* (M.I.T., Mass, U.S.A, January 1985).
7. C. Pegard, "Coordination of autonomous mobile robots" (in French) *PhD. Thesis* (University of Picardie, France, December 1988).
8. Roger Y. Tsai, "A versatile camera calibration technique for high-accuracy 3D machine vision metrology using off the shelf TV camera lenses", *IEEE Journal of Robotics and Automation* **R.A.-3**, No. 4, 323–344 (1987).
9. G. Florou and R. Mohr, "What Accuracy for 3D Measurements with Cameras". *Rapport Interne* (GRAVIR, Grenoble, France, December 21, 1995).
10. G. Toscani "Système de calibration et perception du mouvement en vision artificielle," *Thèse de doctorat* (l'université de Paris Sud, Centre d'Orsay, 1987).
11. John J. Leonard and Hugh F. Durrant-Whyte, "Mobile robot localization by tracking geometric beacons", *IEEE transactions on Robotics and Automation*, **7**, No. 3, 89–97 (June, 1991).
12. Caterpillar, "Caterpillar self guided vehicle systems" *Manufacturer documentation* (in French, 1992).

https://doi.org/10.1017/S0263574799001927 Published online by Cambridge University Press